



## 32 1. INTRODUCTION

33 The most basic form of travel between 2 points in a country corresponds to roads and highways. These are  
34 key to a country's economic and social development [1], [2]. As a reference, approximately 95% of road and  
35 highway pavements around the world correspond to asphalt pavements [3]. Additionally, pavement structure  
36 is the part of the road infrastructure which requires the greatest investment of economic resources, both in the  
37 construction and maintenance stages [4]. Furthermore, the pavement state directly influences the majority of  
38 indirect highway costs. These costs increase when the pavement state is not optimal, mainly due to increases  
39 in travel times, fuel consumption, and deterioration of transportation vehicles, among others [5], [6]. In the  
40 case of asphalt mixtures, the main performance properties that should be considered during dosage and design  
41 phases are: 1) resistance to plastic deformations, 2) resistance to raveling due to damage caused by moisture,  
42 3) resistance to thermal stress cracking, and 4) resistance to fatigue cracking. This last property refers to the  
43 resistance that an asphalt mixture must present when subjected to the dynamic and repetitive solicitations  
44 caused by traffic loads. In this aspect, it is important to highlight that distress caused by fatigue cracking of  
45 the asphalt mixture layers is one of the main damage mechanisms that take place in asphalt pavements [7],  
46 [8]. The accelerated progress of fatigue cracking involves serious economic implications, mainly due to the  
47 need to rehabilitate or rebuild pavement structure before the estimated time, thus increasing the cost of  
48 infrastructure at the time of use. Additionally, this distress has an aesthetic effect when rehabilitation is not  
49 carried out in the indicated period, or when only minor maintenance is done. Finally, there is an effect on  
50 comfort for road users, which also affects their safety due to possible structure detachments when  
51 deterioration is greater [5], [9]. Fatigue cracking is caused by tensile and compressive forces produced by the  
52 traffic loads on the pavement, leading to the progressive reduction of asphalt mixture stiffness modulus [10].  
53 In a pavement structure, when the vehicle wheel loads are relatively far from the considered cross section, a  
54 tensile force is produced at the top of the layer and a compressive force is produced at the bottom, Fig 1a.  
55 Then, when the load is on top of the considered section, the stress state changes, and a compressive force is  
56 produced at the top of the layer while a tensile force is produced at the bottom. After the load passes, the  
57 stress state reverses again [11]. This effect is continuously repeated with the passing of each vehicle over the  
58 pavement. In this context, asphalt mixtures work as a dual system of mechanical resistance: on one hand,  
59 during compression the friction between the mineral particles oppose its relative displacement, on the other

60 hand, during tension the binder and interlocking of aggregates resist the stresses. For these reasons, good  
61 adhesion between the aggregates and binder (even in the presence of water) and sufficient internal cohesion in  
62 the mixture (so that the binder does not break) are the properties desired for a good performance of the asphalt  
63 mixtures [12].

64 In the traditional approach to fatigue cracking in asphalt mixtures, bottom-up cracking is considered. That is,  
65 micro-cracks are caused by deformations from tensile stresses originated in the lower part of the asphalt layer,  
66 causing the beginning of the crack and its propagation towards the surface. Regarding this, the repetition and  
67 accumulation of loads generate cracking and the consequent failure due to pavement fatigue, despite stresses  
68 generated are lower than the tensile stress limit of the material [13], [14]. In addition to the traditional  
69 approach, there are also several studies indicating that there is a top-down cracking mechanism which  
70 collaborates in fatigue cracking produced by thermal variations and by heavy vehicles with high tire inflation  
71 pressure, thus generating tensile and shear stresses on the pavement surface [15], [16].

72 As a consequence of the traffic loads asphalt mixtures accumulate damage, which results in a gradual  
73 cracking process instead of a sudden process of brittle failure. From this point of view, the validity of Miner's  
74 Law is often supported for fatigue analysis, establishing that each applied load generates fatigue consumption,  
75 and that these consumptions accumulate until the fatigue resistance of the mixture is exhausted [17], [18],  
76 [19]. In this context, Kanitpong and Bahía pointed out that during the fatigue process, the continuous loss of  
77 resistance and degradation of the asphalt mixture is a result of the formation of initial microcracks and the  
78 consequent accumulation of damage that achieves the total degradation of the material [20]. This concept is  
79 expressed more clearly by Baaj and Di Benedetto, who noted that the fatigue degradation process of an  
80 asphalt mixture can be established in three phases, which are: 1) phase I or adaptation phase, which is  
81 characterized by the beginning of microcracking, producing a sharp decrease in the dynamic modulus, which  
82 is not only attributed to a fatigue phenomenon, but rather to a combined phenomenon resulting from material  
83 thixotropy and initial heating due to the test's application of cyclic loading, 2) phase II or fatigue phase, is  
84 mainly characterized by fatigue deterioration in the damage evolution of the mixture. Macrocracks resulting  
85 from the union of microcracks generated in phase I appear. This phase is characterized by a linear decrease of  
86 the stiffness with the number of cycles. Finally, 3) phase III or failure phase, in which the macrocracks  
87 quickly progress until the total failure of the asphalt mixture occurs [21].

88 Nowadays, asphalt mixtures' resistance to fatigue cracking is determined in the laboratory by applying  
89 repeated loading to specimens [8], [22]. These procedures consist of conducting cyclic tests at constant stress  
90 or strain amplitude, and using the classic failure criterion. This failure criterion, as described in the European  
91 standard UNE-EN 12697:24, establishes failure of the specimen when its stiffness reduces half of the initial  
92 value. In the case of displacement or strain-controlled tests, the failure of the specimen is assumed when the  
93 initial load ( $F_0$ ) is reduced by half ( $F_0/2$ ), and in the case of force or stress-controlled tests, failure of the  
94 specimen is assumed when the strain ( $\epsilon_0$ ) is equal to double the initial strain ( $2\epsilon_0$ ) [23]. However, one of the  
95 disadvantages that arise in these procedures is that their failure criteria provide erroneous results when testing  
96 very flexible asphalt mixtures, manufactured using a high content of asphalt binder or modified binders.  
97 These flexible mixtures can experience a 50% reduction in their stiffness only due to reversible phenomena,  
98 and therefore not fail if solicitation is reduced or completely stopped [24]. This is explained due to a  
99 readjustment of the materials into the mixture, mainly due to material viscoelasticity. A combined effect of  
100 thixotropy and heating may exist due to the application of dynamic loads; once the application of these  
101 dynamic loads has finished, the material recovers part of its condition or original state [25], [26], [27], [28]. It  
102 has also been observed that when stress-controlled determination tests are conducted, fatigue failure takes  
103 place at the same strain level regardless of the level of applied stress [29]. This indicates that there is a strain  
104 level at which each asphalt mixture fails under cyclic loading in stress-controlled tests. This strain would  
105 correspond to the strain amplitude that would cause failure in few cycles in cyclic strain-controlled tests.  
106 Moreover, there is a stress level below which the mixture presents elastic behavior and the applied loads do  
107 not produce any distress process [17], [30], [31]. In this context, it is very important to know these two strain  
108 levels to characterize the behavior of the material under cyclic loading: 1) the level that does not produce  
109 damage, and 2) the level which causes total failure in few load applications.

110 In relation to the procedures that are used to characterize resistance to fatigue cracking in asphalt mixtures,  
111 these present some drawbacks which cause that the fatigue property of asphalt mixtures is usually not  
112 considered in asphalt mixtures design. The main one being that these tests require extended periods of time  
113 for test execution and numerous tests (and specimens) to characterize the material (e.g. the UNE EN 12697-  
114 24 standard requires 6 replicates to be tested at three strain amplitudes, a total of 18 replicates) [32]. To  
115 overcome this, some testing procedures or prediction models have been developed recently to predict fatigue

116 behavior of asphalt mixtures in a shorter period of time [8], [33], [34], [35]. An example is the Fenix  
117 procedure. Using some of the parameters obtained in this test procedure, a fatigue law can be estimated [36].  
118 Another procedure that provides a faster way of obtaining an estimation of the fatigue law of the asphalt  
119 mixtures is the EBADE test [37], [38], which is based on a strain sweep imposed on a notched prismatic  
120 specimen. This procedure accelerates the damage process in the material by increasing the strain applied,  
121 providing an overall view of its behavior under cyclic loading at different strain amplitudes in a single test.  
122 Although these methodologies (Fenix and EBADE) are good procedures to estimate the fatigue response of  
123 asphalt mixtures in the short term, a better procedure could be developed keeping in mind that, 1) the Fenix  
124 test was designed to evaluate mechanical cracking resistance of asphalt mixtures in the face of static load  
125 application at direct tension (it is not a dynamic fatigue test), and whose correlations were obtained for a  
126 specific number of asphalt mixtures in specific environmental conditions [36], and 2) a study carried out by  
127 Tangella et al. that indicated the stress-controlled fatigue tests present advantages over strain-controlled tests,  
128 including: lower dispersion of results, shorter time test execution and the results reflect a greater influence of  
129 the mixture characteristics, among others [39].  
130 The purpose of the present paper is to present the application of a new stress sweep fatigue test method  
131 developed at the University of La Frontera, called DUSST (Direct Uniaxial Stress Sweep Test), with the aim  
132 of improving the main drawbacks related to the conventional and non-traditional test methods and its failure  
133 criteria, previously described. This fatigue test method tries to represent the main stress state at which the  
134 asphalt mixture is subjected in the pavement structure.

135

## 136 **2. DUSST TEST DEVELOPMENT**

### 137 **2.1 Description of the test device, specimen and procedure**

138 The Direct Uniaxial Stress Sweep Test (DUSST) simulates the cyclical tension-compression stresses that  
139 occur both in the surface area and at the base of the asphalt layers of the pavement, Fig.1a. To this end,  
140 cylindrical specimens are manufactured by extraction of a cylindrical core with a diameter of 50.8 mm (2  
141 inches), from samples fabricated by standard manufacturing methods, such as the Marshall method or the  
142 gyratory compactor. It can also be obtained from field cores extracted from the pavement. The cylindrical  
143 cores are extracted so their vertical axis is perpendicular to the compaction direction. Afterwards, the ends of

144 the extracted core are cut to produce parallel faces and a diametric notch of 5 mm deep and 4 mm wide is  
145 made in the central area. Its height, which can range from 60 to 120 mm, depends on the diameter of the test  
146 piece or field core of origin (often 100 or 150 mm), Fig 1b. For the execution of the test, the specimen must  
147 be fixed between two metal plates, which must be parallel between their faces for the correct axial application  
148 of the forces. Then, the specimen is fixed to a dynamic press and two sensors that are used to record the  
149 deformations of the specimen during the execution of the test, Fig 2a. On the specimen, a series of 5000  
150 cycles of incremental stresses is applied uniaxially with a sinusoidal traction-compression signal in each  
151 cycle, Fig 2d. For each cycle the level of deformation of the specimen is recorded. This is done until the test  
152 piece breaks due to fatigue. This rupture occurs in the area of the specimen previously notched due to the  
153 higher stress concentration, Fig 2b and Fig 2c. Throughout the test period, the evolution of the module and the  
154 energy dissipated are recorded. The test can be carried out at different frequencies and temperatures. For this  
155 procedure, two levels of deformation, that define the fatigue behavior of the mixture, have been established  
156 [32]. The failure strain ( $\epsilon_f$ ) is defined as that which would cause the failure of the material in few load  
157 applications and is measured as the double of the average strain recorded during the cycles 100 and 500 of  
158 each loading stage. The initial strain ( $\epsilon_i$ ) is defined as the one that would produce the failure in a very high  
159 number of load applications (associated with the endurance limit). This strain value is obtained as the average  
160 strain of the previous step to that in which the difference of the average of strain between cycles 100 and 500,  
161 and cycles 4600 and 5000, is less than 10%, Fig. 3.

## 162 **2.2 DUSST parameters**

163 During the test load and vertical displacement are measured continuously and from them stress ( $\sigma$ ) in MPa,  
164 strain ( $\epsilon$ ), norm of the complex modulus ( $|E^*|$ ) in MPa and dissipated energy density (DED) in  $J/m^3$  are  
165 computed using equations (1-4):

$$\sigma = \frac{F}{A_f}, \quad (1)$$

166

$$\epsilon = \frac{\Delta L}{A_f} \cdot \left( \frac{Li}{1013.42} + \frac{4}{A_f} \right), \quad (2)$$

167

168

$$|E^*| = \frac{\sigma_{max}}{\varepsilon_{max}}, \quad (3)$$

169

$$DED = \frac{1}{2} |(\sigma_1 \varepsilon_2 + \sigma_2 \varepsilon_3 + \dots + \sigma_{n-1} \varepsilon_n + \sigma_n \varepsilon_1) - (\sigma_2 \varepsilon_1 + \sigma_3 \varepsilon_2 + \dots + \sigma_n \varepsilon_{n-1} + \sigma_1 \varepsilon_n)| \cdot 10^6, \quad (4)$$

170

171 where,  $F$  is the force in N,  $A_f$  is the area of the notched section of the specimen in  $\text{mm}^2$ ,  $\Delta L$  is the change in

172 length,  $L_i$  is the half of the measurement length less the half of the notch length,  $\sigma_{max}$  is the stress amplitude in

173 a cycle,  $\varepsilon_{max}$  is the strain amplitude recorded during the same cycle,  $\sigma_i$  and  $\varepsilon_i$  are the  $n$  values of stress and

174 strain recorded within the cycle  $i$ .

### 175 3. EXPERIMENTAL STUDY

176 The purpose of this section is to show the application of the DUSST procedure as well as the results that can

177 be obtained from it. The experimental plan and the materials used during this investigation are described. The

178 results obtained and their implications regarding the fatigue behavior of the mixtures studied are presented.

179 Finally, a statistical analysis to evaluate the sensitivity of the parameters delivered by the proposed procedure

180 is presented.

#### 181 3.1 Materials and testing plan

182 In this study, the DUSST procedure was applied to five semi-dense asphalt mixtures type IV-A-12 (according

183 to the Chilean specification), whose granulometry is shown in Fig 4. Three types of asphalt binders and three

184 types of aggregates were evaluated. The asphalt cements used corresponded to a conventional binder, CA-24;

185 an SBS polymer modified binder, CA-PM; and a high modulus asphalt binder, CA-HM, which is

186 characterized by its low penetration and by being used for the manufacture of high modulus mixtures, Table

187 1. The aggregates used were 2 fluvial type (AF1 and AF2) and one coming from quarry (AC). The fluvial

188 type aggregates were obtained from the same place and they are mainly composed of dolomite, basalt, dacite,

189 andesite, rhyolite, sandstone, quartz and quartzite. The quarry aggregate AC is composed mainly of quartz,

190 biotite and iron oxide. The only difference between fluvial aggregates is the crushing process. AF1 was

191 obtained by means of a cone crusher and AF2 was obtained by an impact crusher. The AC aggregates were

192 obtained by means of a cone crusher. The characteristics of the aggregates used can be seen in Table 2.

193 The asphalt mixtures used to evaluate the effect of the type of binder were manufactured with the aggregate

194 AF1, while those employed to evaluate the effect of the type of aggregate were fabricated using the

195 conventional binder CA-24. The optimum binder content for all mixtures evaluated was 5.2% on aggregates  
196 weight, and it was obtained by means of Marshall Design Method, according to Chilean specifications. The  
197 dimensions of the DUSST specimens used in this study were 50.8 mm in diameter, 60 mm in height and a  
198 notch in the central area of 4 mm in height and 5 mm in depth. These DUSST specimens were extracted from  
199 100 mm diameter cylindrical samples manufactured by the Marshall method. The test routine consisted in the  
200 application of series of cycles of different stress amplitudes, with a duration of 5,000 cycles each. It started  
201 with a stress amplitude of 250 kPa and the amplitude was increased by 50 kPa every 5,000 cycles until the  
202 material failed. Three specimens were evaluated for each type of mixture, the frequency of the stress input  
203 signal was 10 Hz during the whole test and the test temperature was 20°C. The strain amplitude, the norm of  
204 the complex modulus  $|E^*|$ , the dissipated energy density, DED, the failure strain and the initial strain were  
205 obtain for each specimen. To evaluate the sensitivity of the procedure in relation to the variables type of  
206 binder and type of aggregate, an ANOVA analysis of variance was performed. For each parameter delivered  
207 by the DUSST test, a variance analysis of one factor with several samples per group was performed. For these  
208 analyzes the factors evaluated were: type of binder and type of aggregate. The binder type factor consisted of  
209 three levels corresponding to the three binders analyzed (CA24, CA PM, CA HM), while for type factor of  
210 aggregate, consisted of three levels (AF1, AF2 and AC).

## 211 4. ANALYSIS OF THE RESULTS

### 212 4.1 Evolution of strains

213 Figure 5 shows the evolution of the strain during the tests for the mixtures manufactured with different  
214 binders. The strain increased gradually, showing higher slopes as the stress applied increased until the  
215 specimens failed. The mixture made with the polymer-modified binder, CA-PM, showed greater ductility,  
216 showing higher initial and failure strains than the mixtures manufactured with CA-24 and CA-HM. In  
217 addition, it recorded a greater number of cycles until the material failed, indicating that it resisted a higher  
218 stress amplitude. On the other hand, the more rigid mixture manufactured with the high modulus binder, CA-  
219 HM, registered low levels of initial and failure strains ( $\epsilon_i$  and  $\epsilon_f$ ), with the smallest difference between these  
220 two values. Therefore, the slope change in the strain vs. cycle curve between stress levels was very small. The  
221 mixture made with the conventional binder CA 24 showed a more ductile behavior than the high modulus  
222 one, showing higher initial and failure strains.

223

224 Unlike other standardized procedures, the DUSST was able to show clearly the strain amplitude at which the  
225 asphalt mixture fails in stress-controlled cyclic testing, regardless of the stiffness of the mixture. The two  
226 strain values obtained in the test ( $\epsilon_i$  and  $\epsilon_f$ ) can be related with the fatigue law of the mixture. The initial strain  
227 is related with a strain level at which the mixture could endure millions of cycles in a conventional time  
228 sweep test, i.e., the endurance limit. Regarding the failure strain, this value should be related with the strain at  
229 which the mixture would reach failure in a few thousand cycles in time sweep test. Previous research using  
230 strain sweep test [Botella, R., Pérez-Jiménez, F.E., Miro, R., Martínez, A.H. New methodology to estimate  
231 the fatigue behavior of bituminous mixtures using a strain sweep test (2017) Construction and Building  
232 Materials, 135, pp. 233-240. López-Montero, T., Miró, R., Botella, R., Pérez-Jiménez, F.E. Obtaining the  
233 fatigue laws of bituminous mixtures from a strain sweep test: Effect of temperature and aging (2017)  
234 International Journal of Fatigue, 100, pp. 195-205.] showed failure strain correlated fairly well with the strain  
235 level that produced failure in time sweep tests in 10,000 cycles, and that fatigue laws obtained in time sweep  
236 tests predicted 10 million cycles for strains close to the failure strain. Following this line of research, time  
237 sweep tests results were analyzed and compared with the DUSST results leading to the conclusion that the  
238 initial strain obtained from DUSST corresponds to 5,000 cycles and the failure strain to 50 million cycles in  
239 time sweep tests at those strain levels. Therefore, a rough approximation to the fatigue law of the material was  
240 extracted from the DUSST results pairing 5,000 cycles with the initial strain and 50 million cycles with the  
241 failure strain. The fatigue laws obtained by this methodology are shown in figure 5.

242

243 Regarding the influence of the aggregate type, table 3 shows the average parameters obtained in the DUSST  
244 for each mixture. These results show that the mixture manufactured with the aggregate with the highest form  
245 factor and lowest slab index (AF2), Table 2, obtained greater number of cycles until failure, showing a higher  
246 initial strain, but failed at lower failure strain. Conversely, the mixture with the aggregate with the highest rate  
247 of slabs and the lowest values registered in the form factor and fine particle index (AC) presented a lower  
248 durability. The mixture made with the aggregate AF1 with intermediate values in its form factor, slab index  
249 and Fine particle index, recorded an intermediate durability, but with a greater difference between the values  
250 of initial and failure strain.

251 **4.2 Evolution of complex modulus**

252 The evolution of the complex modulus ( $|E^*|$ ) during the test is shown in Figure 6. The most rigid mixture,  
253 manufactured with the CA-HM binder, obtained the highest initial modulus value ( $|E^*|_i$ ), 10,790 MPa. In  
254 this case, the material behaves elastically to a high level of stress, but its degradation occurs more abruptly  
255 than the other mixtures evaluated. On the contrary, the value of the initial complex modulus of the mixture  
256 made with the polymer-modified binder (CA-PM) was 4,600 MPa. Figure 6 shows that for this mixture the  
257 deterioration was continuous and progressive as the stress level increased, but without an abrupt failure.  
258 Además, registró la menor pendiente de daño del material entre las mezclas evaluadas. The mixture with the  
259 conventional binder CA-24 showed an intermediate behavior, with an initial complex modulus value ( $|E^*|_i$ ) of  
260 6,788 MPa. A continuous decrease of stiffness was observed during the test. Regarding the influence of the  
261 aggregate type (Table 3), it is observed that the mixtures with the highest value of Coarse particle index  
262 (Table 2) obtained higher initial complex modules ( $|E^*|_i$ ), which agrees with what was expressed in a  
263 previously published study [40].

264 **4.3 Evolution of dissipated energy**

265 The dissipated energy during each cycle was computed as the area of the hysteresis loop that forms in the  
266 stress-strain plane. As the stress amplitude applied increased, also did the strain amplitude, and therefore the  
267 hysteresis loop area and the dissipated energy. The dissipated energy density recorded in each cycle ( $DED_c$ )  
268 and the accumulated dissipated energy density during the whole test ( $DED_a$ ) are shown in figure 7. The values  
269 obtained from accumulated dissipated energy ( $DED_a$ ) were 9,791 MJ /m<sup>3</sup>, 2,817 MJ / m<sup>3</sup> and 0.543 MJ / m<sup>3</sup>  
270 for the mixtures manufactured with the binders CA-PM, CA-24 and CA-HM, respectively. The mixture that  
271 showed the best behavior is the one manufactured with the polymer modified binder, CA-MP, dissipating  
272 around 18 times more energy in the whole fatigue process than the more rigid mixture with the CA-HM  
273 binder and almost 3.5 times more than the mixture made with the conventional binder CA-24. Regarding the  
274 aggregate type study, it was observed that those mixtures with higher number of cycles to failure (AF1 and  
275 AF2) obtained the highest values of accumulated dissipated energy ( $DED_a$ ). However, among them, a mixed  
276 effect between ductility and durability was observed, which led to similar values of accumulated dissipated  
277 energy ( $DED_a$ ), Table 3. The accumulated dissipated energy parameter ( $DED_a$ ), defined in the DUSST test  
278 method, is considered an important and promising parameter to characterize the fatigue behavior of the

279 asphalt mixtures, since it provides a relation between the work required to achieve the failure of the mix and  
280 the degree of ductility that it has.

281

#### 282 **4.4 Statistical analysis of results**

283 Sensitivity of the DUSST test was evaluated by a variance analysis (ANOVA) of the results for the most  
284 relevant parameters obtained in the experimental tests. With ANOVA it is possible to find out whether the  
285 values of a set of numerical data are significantly different from those of other sets. Thus, test sensitivity for a  
286 specific parameter can be determined. In a first stage, test sensitivity of the IV-A-12 mixture to binder type  
287 was analysed from the results obtained for the initial strain ( $\epsilon_i$ ), failure strain ( $\epsilon_f$ ), complex modulus ( $|E^*|_i$ ) and  
288 dissipated energy ( $DED_a$ ). A variance analysis of one factor (i.e., binder type) was conducted with several  
289 samples per group. Binder type levels were CA-24, CA-PM and CA-HM, with three data for each level. As  
290 can be seen at the top of the Table 4, the F-Value for binder type factor for all evaluated parameters are  
291 greater than their critical values determined for a significance level of 0.05. This means that for the binder  
292 type, significantly different values are obtained for the evaluated DUSST parameters. Thus, test sensitivity to  
293 the factor analysed at this stage is determined. Analogously, in a second stage, test sensitivity of the IV-A-12  
294 mixture to aggregate type was analysed for the same DUSST parameters. As in the previous stage, a variance  
295 analysis of one factor (i.e., aggregate type) was carried out with several samples per group. Aggregate type  
296 levels were AC, AF1 and AF2, with three data for each level. From the Table 4, it can be concluded that, for  
297 aggregate type, significantly different values of most of the evaluated parameters are obtained in the DUSST  
298 tests. Thus, test sensitivity to the factor analysed at this stage is determined.

#### 299 **5. CONCLUSIONS**

300 The following conclusions can be drawn from the results of this study:

- 301 1. The DUSST proved to be a practical method with great potential to characterize fatigue behavior of  
302 asphalt mixtures in a shorter time as far as variables such as binder type and aggregate type are  
303 concerned. In addition, this test can be used on laboratory specimens and on field cores.
- 304 2. The DUSST produced important parameters to characterize the fatigue behavior of asphalt mixture,  
305 such as: initial strain, failure strain, complex modulus and dissipated energy. Moreover, it provided

306 reliable failure criterion that characterize the fatigue damage of the mixture, and helped classify them  
307 as being ductile or stiff.

308 3. A fatigue law estimation was proposed using the DUSST. This test does not seek to replace the  
309 cyclic tests to obtain fatigue test laws. Rather, it proposes a new tool to quickly estimate the fatigue  
310 behavior of asphalt mixtures.

311 4. Good sensitivity of the DUSST test to variables tested have been determined by ANOVA of the  
312 results of the main parameters of the new test procedure.

### 313 **6. ACKNOWLEDGEMENTS**

314 The present paper is the result of the research supported by Universidad de la Frontera program, conducted  
315 within the framework of the Project DI18-0053.

316

## REFERENCES

- [1] T. Keane, "The economic importance of the national highway system," *Public Roads*, vol. 59, no. 4, 1996.
- [2] H. Ibarrola, "La importancia de la infraestructura carretera en el desarrollo económico de un país.," *Rutas*, pp. 2-3, 2008.
- [3] Asphalt Institute, *The Asphalt Handbook. MS-4. 7th edition.*, USA: Asphalt Institute, 2007.
- [4] Y. Huang, *Pavement Analysis and Design (2nd Edition)*, New Jersey: Pearson Prentice Hall, 2004.
- [5] H. De Solminihaç, *Gestión de Infraestructura Vial*, Santiago: Pontificia Universidad Católica de Chile, 2001.
- [6] F. Pérez, R. Miró and A. Martínez, *Proyecto y conservación de carreteras.*, Barcelona: Asociación Española de la Carretera., 2006.
- [7] H. Di Benedetto, C. De la Roche, H. Baaj and A. Pronk, "Fatigue of bituminous mixtures: different approaches and RILEM group contribution.," in *Sixth international RILEM Symposium on Performance Testing and Evaluation of Bituminous Materials*, Zurich, 2003.
- [8] F. Moreno and M. Rubio, "UGR-FACT test for the study of fatigue cracking in bituminous mixes.," *Construction and Building Materials*, vol. 43, pp. 184-190, 2013.
- [9] G. Valdés, F. Pérez, R. Miró, A. Martínez and J. Amoros, "Desarrollo de un nuevo ensayo experimental para la evaluación de la resistencia a tracción directa y la energía disipada en el proceso de fractura en mezclas asfálticas.," in *XV CILA Congreso Iberoamericano del Asfalto*, Lisboa, 2009.
- [10] K. Mollehauser and M. Wistuba, "Fatigue effect in uniaxial cyclic stress test: The link between stiffness decrease and accumulation of irreversible strain.," in *7th International RILEM Symposium on Advanced Testing and Characterization of Bituminous Materials*, Greece, 2009.
- [11] C. Racanel, M. Romanescu, M. Dicu, A. Burlacu and C. Surlea, "Fatigue lines for asphalt mixtures used in wearing course.," *Advanced Testing and Characterization of Bituminous Materials*, vol. 2, pp. 795-805, 2009.
- [12] F. Moreno, *Diseño de un método de ensayo de laboratorio para el análisis de la resistencia a fisuración*

de mezclas bituminosas utilizadas en la construcción de firmes de carretera., Granada: Tesis Doctoral. Universidad de Granada., 2012.

- [13] F. Pérez, R. Miró, A. Martínez, J. Alonso, J. Cepeda and M. Rodríguez, Desarrollo de un nuevo procedimiento para la evaluación del comportamiento a fatiga de las mezclas bituminosas a partir de su caracterización en un ensayo a tracción., Madrid: Premio Internacional a la Innovación en Carreteras Juan Antonio Fernández del Campo., 2005.
- [14] R. Brown, P. Kandhal and J. Zhang, "Performance testing for hot mix asphalt. NCAT Report 01-05.," National Center for Asphalt Technology., Auburn, 2001.
- [15] D. Harmelink and T. Aschenbrener, "Extent of top-down cracking in Colorado, Report No. CDOT-DTD-R-2003-7.," Colorado Department of Transportation., Denver, 2003.
- [16] H. Yared, D. Jelagin and B. Birgisson., "Mechanics-based top-down fatigue cracking initiation prediction framework for asphalt pavements.," *Road Materials and Pavement Design*, vol. 16, pp. 907-927, 2015.
- [17] S. Carpenter, "Fatigue Performance of IDOT Mixtures. Research Report FHWA-ICT-07-007.," Illinois Center for Transportation, Rantoul, 2006.
- [18] J. González, J. Canet, S. Oller and R. Miró, "A viscoplastic constitutive model with strain rate variables for asphalt mixtures- numerical simulation," *Computational Material Science*, vol. 38, pp. 543-560, 2006.
- [19] R. Lugmayr, M. Jamek and E. Tshogg, "Mechanism of fatigue crack growth and fracture behavior in bituminous roads," *Advanced Testing and Characterization of Bituminous Materials*, vol. 2, pp. 807-816, 2009.
- [20] K. Kanitpong and H. Bahia, "Relating adhesion and cohesion of asphalts to the effect of moisture on laboratory performance of asphalt mixtures," *Transportation Research Record*, vol. 1901, pp. 33-43, 2005.
- [21] H. Baaj and H. Di Benedetto, "Effect of binder characteristics on fatigue of asphalt pavement using an intrinsic damage approach.," *Road Materials and Pavement Design*, vol. 6, pp. 147-174, 2006.

- [22] S. Zhi, W. Gun, L. Hui and T. Bo, "Evaluation of fatigue crack behavior in asphalt concrete pavements with different polymers modifiers.," *Construction and Building Materials*, vol. 27, pp. 117-125, 2012.
- [23] J. Alonso, Estudio del proceso de deformación y agrietamiento por fatiga de mezclas bituminosas sometidas a carga cíclica., Barcelona: Tesis Doctoral. Universidad Politécnica de Cataluña., 2006.
- [24] F. Pérez, R. Miró, A. Martínez, R. Botella, O. Reyes and G. Valdés, "False failure in flexural fatigue tests.," in *2nd Workshop on 4 PB – Four Point Bending*, Guimaraes, 2009.
- [25] J. Mewis and N. Wagner, "Thixotropy.," *Advances in Colloid and Interface Science*, vol. 147, pp. 214-227, 2009.
- [26] F. Pérez, R. Botella and R. Miró, "Damage and thixotropy in asphalt mixture and binder fatigue tests," *Transportation Research Record: Journal of the Transportation Research Board*, no. 2293, pp. 8-17, 2012.
- [27] R. Botella, F. Pérez, E. Riahi, T. López, R. Miró and A. Martínez, "Importancia de los periodos de reposos en el comportamiento bajo cargas cíclicas de los materiales bituminosos," in *XIX Congreso Ibero Latinoamericano del Asfalto*, Medellín, 2017.
- [28] F. Pérez, R. Botella, R. Miró and A. Martínez, "Analysis of the thixotropic behaviour and the deterioration process of bitumen in fatigue test," *Construction and Building Materials*, vol. 101, pp. 277-286, 2015.
- [29] F. Pérez, R. Miró and A. Martínez, "Analysis of the fatigue process in bituminous mixes.," in *Transportation Research Board. 86th Annual Meeting.*, Washington, 2007.
- [30] H. Von Quintus, "Application of the Endurance Limit Premise in Mechanistic-Empirical Based Pavement Design Procedures.," in *International Conference on Perpetual Pavements*, Columbus, 2006.
- [31] J. García, C. García, J. Buisson, C. Cortés and J. Potti, "Pavimentos de larga duración.," in *VIII Congreso Nacional de Firms.*, Valladolid, 2008.
- [32] UNE-EN 12697-24, *Bituminous mixtures - Test methods for hot mix asphalt - Part 24: Resistance to fatigue*, 2013.
- [33] T. Hou, S. Underwood and R. Kim, "Fatigue performance prediction of North Carolina mixtures using

- the simplified viscoelastic continuum damage model," *Asphalt Paving Technology: Association of Asphalt Paving Technologists-Proceedings of the Technical Sessions*, vol. 79, pp. 35-73, 2010.
- [34] F. Haddadi, M. Ameri, M. Mirabimoghdam and H. Amiri, "Validation of a simplified method in viscoelastic continuum damage (VECD) model developed for flexural mode of loading," *Construction and Building Materials*, no. 95, pp. 892-897, 2015.
- [35] F. Safaei, C. Castorena and Y. Kim, "Linking asphalt binder fatigue to asphalt mixture fatigue performance using viscoelastic continuum damage modeling," *Mechanics of Time-Dependent Materials*, vol. 20, no. 3, pp. 299-323, 2016.
- [36] F. Pérez, G. Valdés, R. Botella, R. Miró and A. Martínez, "Approach to fatigue performance using Fénix test for asphalt concrete mixtures.," *Construction and Building Materials*, vol. 26, no. 1, pp. 372-380, 2012.
- [37] F. Pérez, G. Valdés, R. Miró, R. Botella and J. Campana, "Effect of thermal stresses on fatigue behavior of bituminous mixes.," *Transportation Research Record*, vol. 4, no. 2210, pp. 90-96, 2011.
- [38] R. Botella, F. Pérez, A. Martínez, R. Miró and J. Amorós, "Método de estimación de las leyes de fatiga de las mezclas bituminosas mediante el ensayo Ebade," in *IX Jornada Nacional Asefma*, Madrid, 2014.
- [39] S. Tangella, J. Craus, J. Deacon and C. Monismith, "Summary report on fatigue response of asphalt mixtures. Technical memorandum No. TM-UCB-A-003A-89-3M.," Institute of Transportation Studies, University of California., Berkeley, 1990.
- [40] G. Valdes, A. Calabi, R. Miró and J. Norambuena, "Mechanical behavior of asphalt mixtures with different aggregate type," *Construction and Building Materials*, no. 101, p. 474-481, 2015.



## 7. FIGURES

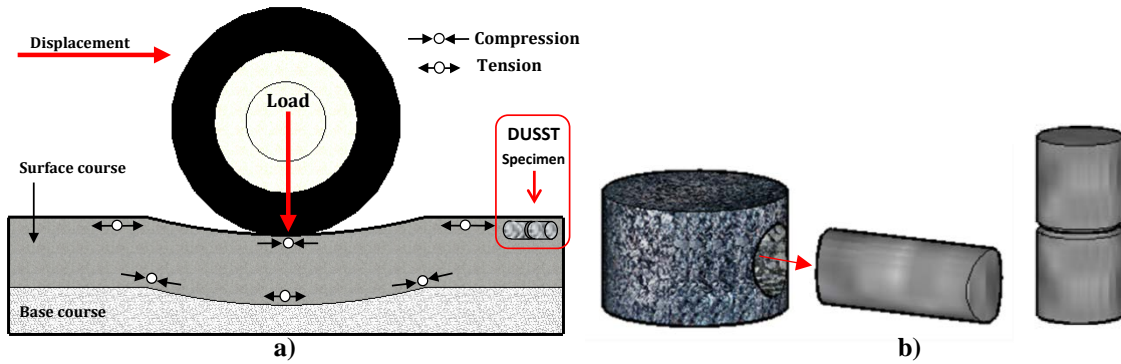


Fig. 1 a) Stress state of the asphalt layers on a pavement and b) DUSST specimen manufacture scheme

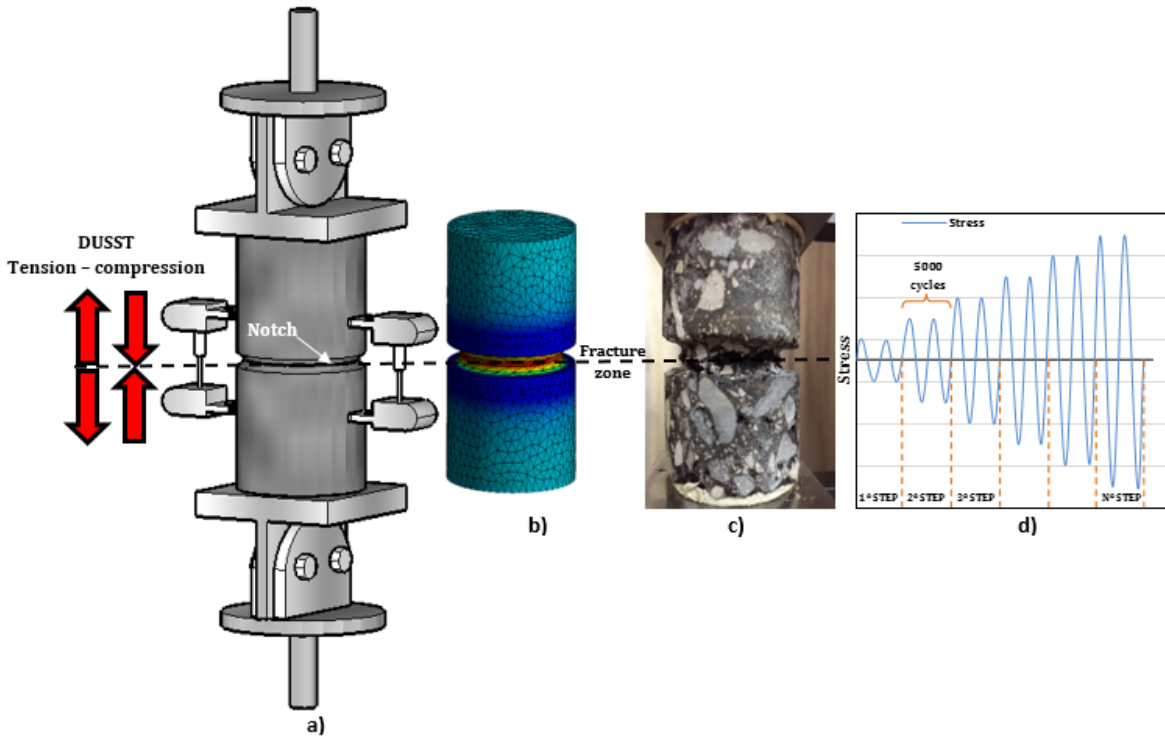


Fig. 2 a) DUSST test device, b) stresses simulation in the test specimen, c) fatigue cracking in the test specimen and d) sinusoidal stresses tension-compression applied to the specimen in DUSST procedure

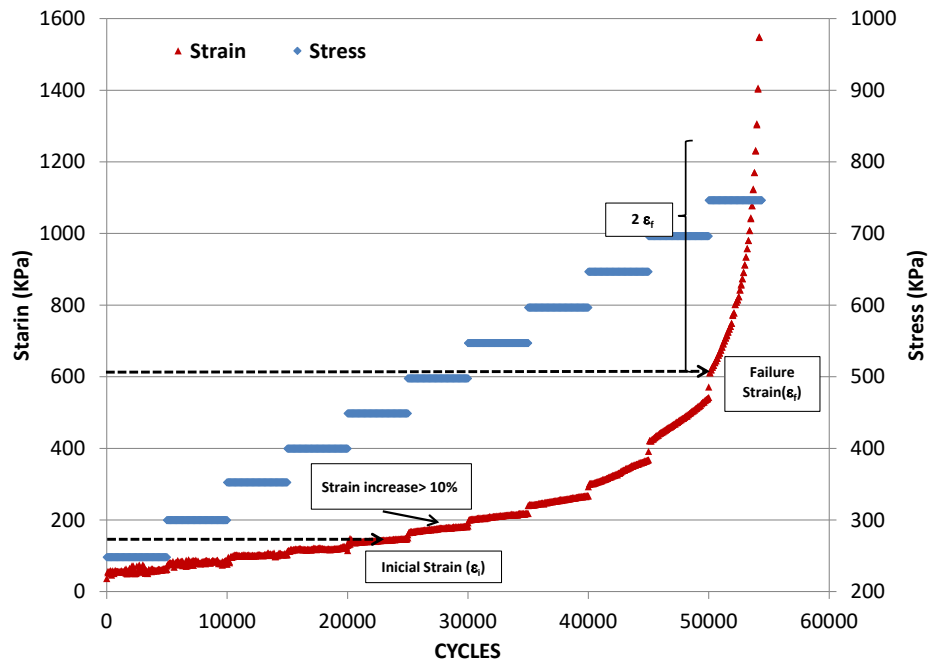


Fig. 3 Evolution of strains evaluated with DUSST procedure

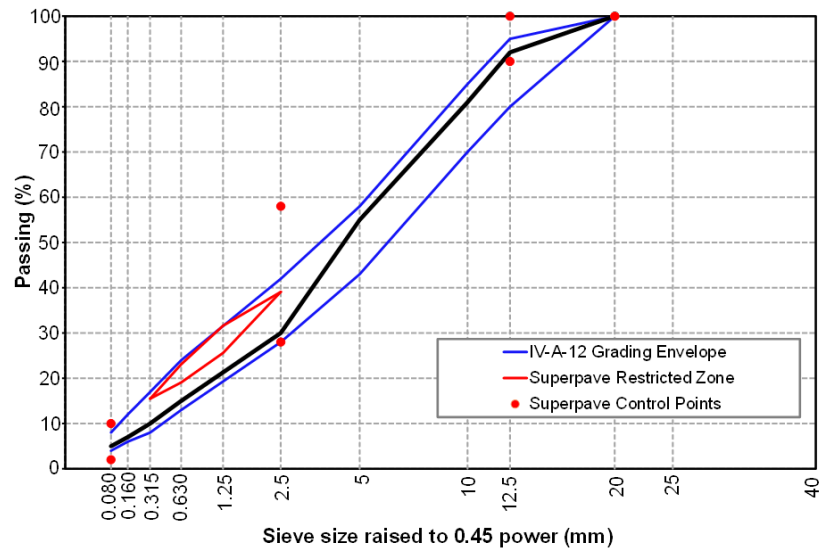


Fig. 4. Aggregate gradation of the IV-A-12 asphalt mixture.

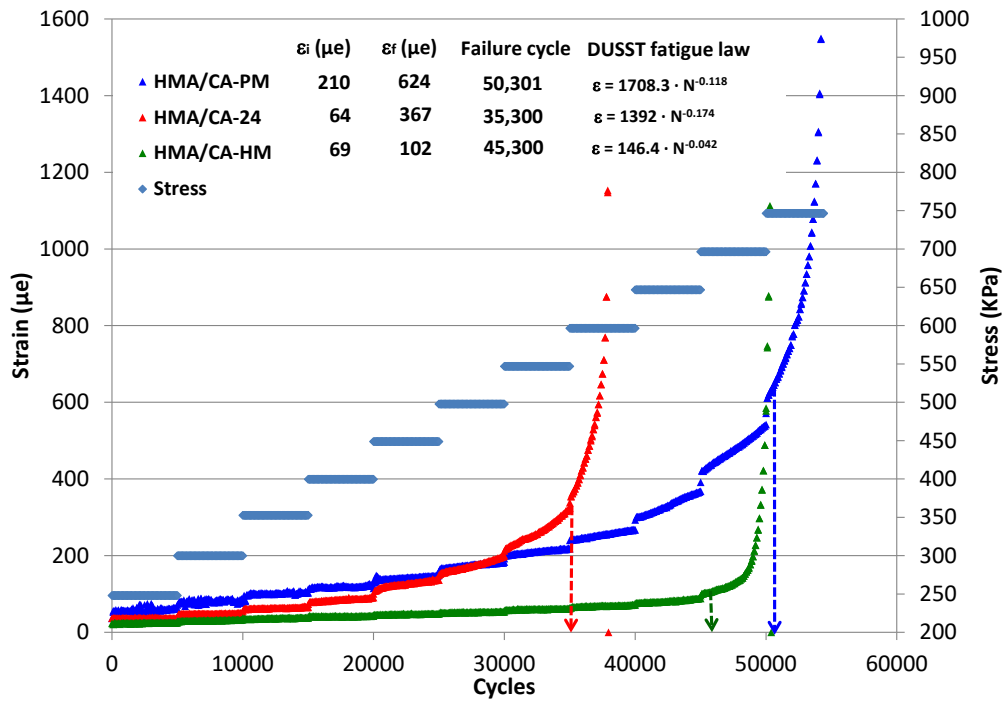


Fig. 5. Evolution of strains in asphalt mixtures with different type of bitumens.

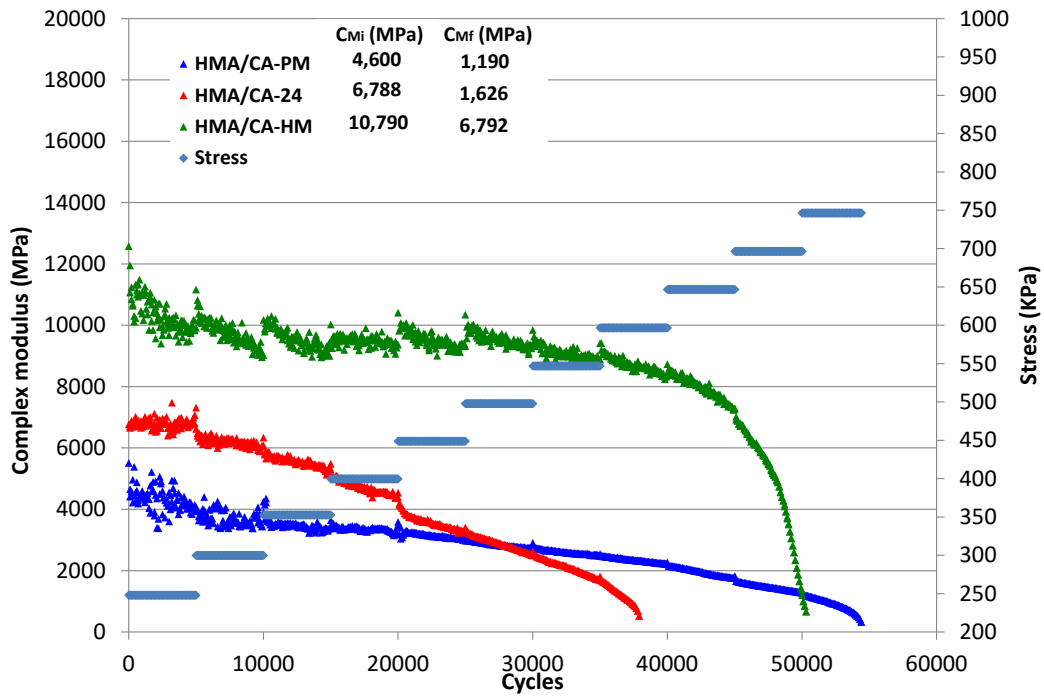


Fig. 6. Evolution of complex modulus in asphalt mixtures with different type of bitumens.

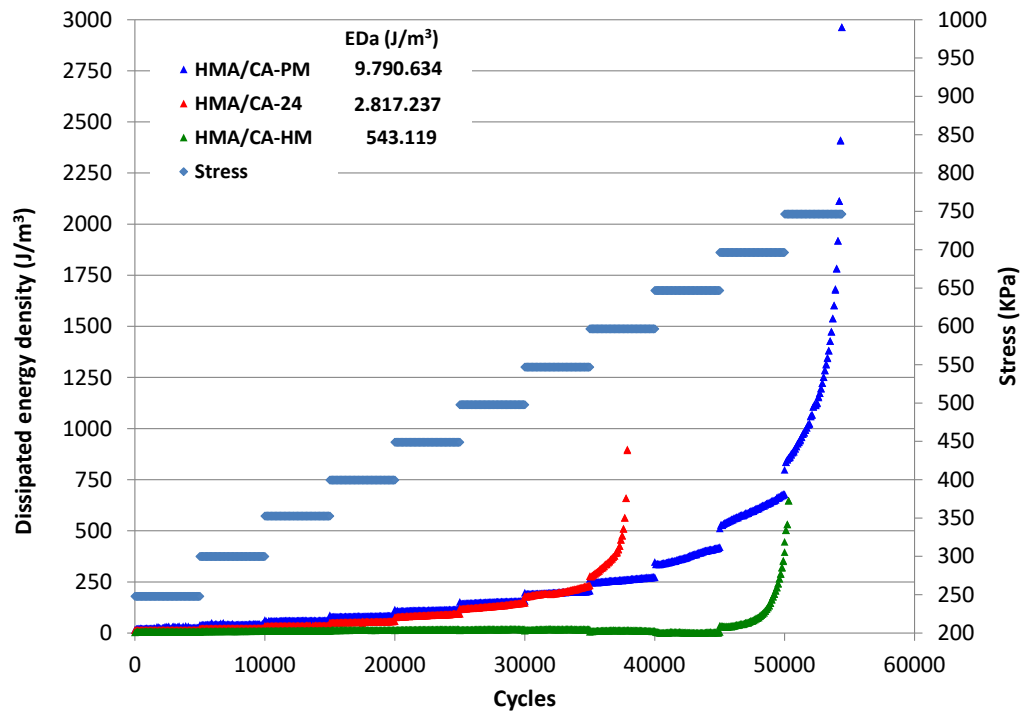


Fig. 7. Evolution of dissipated energy density in asphalt mixtures with different type of bitumens

## 8. TABLES

Table 1. Properties of the bitumens.

Tests	CA-24	Esp.	CA-PM	Esp.	CA-HM	Esp.
Absolute Viscosity at 60°C, 300 mm Hg (P)	3077	Min 2400	-	-	-	-
Penetration at 25 °C, 100 g. 5 s. (0.1 mm)	56	Min 40	65	60-80	14	12-17
Softening Point R&B, (°C)	51	Informar	76	Min 60	65	Min. 65
Ductility at 5°C, (cm)	-	-	52	Min 50	-	-
Ductility at 25°C, (cm)	>150	100	98	Min 80	-	-
Penetration Index	-0.7	-1.5 a +1.0	4.5	Min +2	-0.62	Min. -1.5
Fraass Brittle Point, (°C)	-	-	-18	Max -17	-3	Max. -5
Elastic Recovery (13 °C, 20 cm, 1 hr, %)	-	-	66	Informar	-	-
Cleveland Open Cup Flash Point, (°C)	332	Min 232	240	Min 235	> 240	Min. 240
Brookfield Viscosity at 135°C (cP)	-	-	-	-	1709	Min. 1200
Brookfield Viscosity at 160°C (cP)	-	-	-	-	453.3	Min. 350
Spot test (% xilol)	<25	Max 30	-	-	-	-
Trichloroethylene solubility (%)	99.9	Min 99	-	-	-	-
<b>RTFOT</b>						
Mass Loss, (%).	0.00	Max 0.8	-	-	-	-
Absolute Viscosity at 60°C, 300 mm Hg (P)	7475	Informar	-	-	-	-
Ductility at 25 °C, 5 cm/min, (cm)	150	Min 100	-	-	-	-
Durability Index	2.4	Max 3.5	-	-	-	-
Retained Penetration, (%)	-	-	-	-	64	Min. 55
Softening Point R&B Increase, (°C)	-	-	-	-	9	Max. 10

Table 2. Properties of aggregates.

Tests	AC	AF1	AF2	Specifications
Los Angeles Abrasion Loss (%)	25	16	15	Máx. 25 (*)% - 35%
Crushed aggregates (%)	100	92	90	Mín. 90% (*) - 70%
Flakiness index (%)	8	2,5	0	Máx. 10% (*) - 15%
Specific gravity (kg/m3)	2360	2630	2640	-
Shape factor	0.41	0.52	0.60	-
Coarse particle index	14.4	14.5	12.6	-
Fine particle index	14.1	23.0	17.8	-
Silica by SEM (% weight)	63.3	59.9	59.1	-

(\*) Surface layer

Table 3. DUSST parameters of asphalt mixture manufactured with different type of aggregates.

Aggregate Type	$\epsilon_i$ ( $\mu\epsilon$ )	$\epsilon_r$ ( $\mu\epsilon$ )	Failure Cycle	$ E^* _i$ (MPa)	$ E^* _r$ (MPa)	DED <sub>a</sub> (J/m <sup>3</sup> )
AF1	64	367	35,300	6,788	1,626	2,808,211
AF2	103	271	40,400	6,416	2,349	2,817,237
AC	72	359	30,301	7,612	1,506	2,128,554

Table 4. Results of ANOVA for DUSST parameters

DUSST Parameters	Source of Variation	SS	DF	MS	F-Value	P-Value	Critical F-Value
Initial Strain ( $\epsilon_i$ )	Bitumen type	41131.5556	2	20565.7778	160.53	6.174E-06	5.1432
	Within groups	768.666667	6	128.111111			
Failure Strain ( $\epsilon_f$ )	Bitumen type	408758	2	204379	33.57	0.00055228	5.1432
	Within groups	36534	6	6089			
Complex Modulus ( $E^* _i$ )	Bitumen type	59112653.6	2	29556326.8	37.43	0.00040867	5.1432
	Within groups	4738326.67	6	789721.111			
Dissipated Energy Density ( $DED_a$ )	Bitumen type	1.3932E+14	2	6.9658E+13	63.42	9.2135E-05	5.1432
	Within groups	6.59E+12	6	1.0983E+12			
Initial Strain ( $\epsilon_i$ )	Aggregate type	2577.555556	2	1288.777778	6.12	0.035584317	5.1432
	Within groups	1263.333333	6	210.5555556			
Failure Strain ( $\epsilon_f$ )	Aggregate type	17146.8889	2	8573.44444	5.82	0.0393694	5.1432
	Within groups	8840.66667	6	1473.44444			
Complex Modulus ( $E^* _i$ )	Aggregate type	2246429.56	2	1123214.78	2.59	0.15485535	5.1432
	Within groups	2605484.67	6	434247.444			
Dissipated Energy Density ( $DED_a$ )	Aggregate type	9.363E+11	2	4.6815E+11	5.71	0.0409239	5.1432
	Within groups	4.9231E+11	6	8.2052E+10			